Indian Journal of Pure & Applied Physics
Vol. 56, September 2018, pp. 732-740

Chemical reaction effect on MHD rotating fluid over a vertical plate with variable thermal conductivity: A numerical study

Ram Prakash Sharma[a]*, S M Ibrahim[b], Madhu Jain[c] & S R Mishra[d]

[a]Department of Mathematics, JECRC University, Jaipur 303 905, India

[b]Gitam Institute of Technology, GITAM University, Visakhapatnam 530 045, India

[c]Department of Mathematics, IIT Roorkee 247 667, India

[d]Siksha 'O' Anusandhan University, Khandagiri, Bhubaneswar 751 030, India

Received 12 December 2017; accepted 13 April 2018

In this article, we have considered the simultaneous influence of chemical reaction and heat source on magnetohydrodynamic assorted convective heat and mass transfer flow past a vertical plate in a rotating system. The effects of applied magnetic field have also been taken into consideration while the induced magnetic field has not been reviewed due to very minor magnetic Reynolds number. The governing nonlinear partial differential equations for the flow, energy and species have been changed into highly nonlinear coupled system of ordinary differential equations by the help of similarity transformations and which are then solved numerically by applying fourth order Runge-Kutta technique associated along with shooting technique. The impacts of different variables on the velocity, temperature, concentration, skin friction and rate of heat and mass transfer distribution in the system have been shown graphically and explained in detail. In this paper we differentiate the results with already published works and good concurrence has been acquired to ensure the validity of the study.

Keywords: MHD, Chemical reaction, Heat source, Thermal conductivity, Variable porosity

1 Introduction

Heat and mass transfer issue have a significant effect on modern-day industries, such as catalytic reactors, heat insulation, geothermal systems, drying technology, compact heat exchangers, solar power collectors, paper production and food industries. Mathers *et al.*[1] studied the combined heat and mass transfer in boundary layer flow possess very significant accomplishments in numerous activities and thus gain a considerable amount of observation from contemporary researchers. In various heat and

smaller order of magnitude than the impacts reported by Fourier's and Fick's laws. The Ludwig-thermal diffusion impact corresponds to species differentiation expanding in beginning homogeneous assortment subjected to a temperature gradient. The heat flux impelled through a concentration gradient is called Dufour effect. These impacts are examined as second order phenomena and are remarkable in fields such as chemical reactor, hydrology, petrology, drying processes, geosciences, etc. The impacts of Soret and Dufour effect on the heat and mass transfer were augmented from the kinetic theory of gases by Chapman and Cowling[2]. The investigation of rotating flow with heat transfer has gained huge focus of researchers for applications in planetary sciences and geophysics. The convection heat transfer in a rotating fluid past a vertical plate in a thermally conducting massive very high permeability was studied by Beg *et al.*[3] Al-Humoud *et al.*[4] studied the convective of a rotating fluid past a vertical surface immersed in a thermally conducting massive very huge porous

e convection heat and

sinesq incompressible viscous rotating fluid with chemical reaction and radiative heat transfer have been presented by Mbeledogu and Ogulu[5]. They found that when the values of the radiation and Prandtl number are enhanced, the temperature of the boundary layer decreases. They also found that the flow velocity tends steady state as the time parameter is increased.

The transient incompressible Couette flow in a rotating channel with non-Darcian porous medium was studied by Beg *et al.*[6] Solutions for magnetohydrodynamic rotating flow of a 2-grade fluid with porous medium have been presented by

*Corresponding author (E-mail: ramprakash0808@gmail.com)

Salah *et al.*[7] In general the porosity of the permeable medium considered as constant. Permeability is variable but differs from the wall to the inside because of variation in porosity was studied by Schwartz and Smith[8]. Vafai and Tien[9] have investigated inertia and boundary impacts on flow and heat transfer in the presence of porous media is changeable and constant permeability. They found that the significant effect of the dissimilarity of permeability and porosity occurs in heat transfer and velocity.

The radiation impact on mixed convection past a vertical plate in the presence of variable porosity in porous medium was investigated by Pal and Mondal[10]. MHD non-Darcy combined convection heat transfer from a vertical heated plate inserted in the presence of porous media with variable porosity was investigated by Pal[11]. The thermal radiation impact on MHD natural convection flow of heat and mass transfer with a variable porosity has been presented by Prasad *et al.*[12]. The impact of heat and mass transfer on 2-D MHD free convection flow over a vertical porous plate with the thermal radiation, Dufour and Soret effects in a porous medium have been investigated by Vedavathi *et al.*[13] Alao *et al.*[14] conducted a numerical analysis of the impact of thermal radiation, Soret and Dufour effect on an unsteady heat and mass transfer flow past a vertical plate in the presence of chemical reaction and viscous dissipation.

All the above mentioned studies are restricted to the assumption of constant fluid characteristics. It is notable that the characteristics of fluid may diverge appreciably with temperature. The impact of thermal conductivity and variable viscosity on an unsteady 2-D laminar flow of a viscous incompressible fluid over a vertical porous moving plate in the presence of variable suction and magnetic field was studied by Seddeek and Salama[15].

Mukhopadhyay[16] have carried out numerical solution to the unsteady boundary layer flow and heat transfer over a permeable plate in the presence of thermal diffusivity and variable viscosity. They found that due to increase in unsteadiness parameter, fluid velocity decreases up to the crossing over point and after this point opposite behaviour is noticed. The temperature reduces significantly in this case. Fluid velocity reduces with enhancing temperature-dependent fluid viscosity parameter (i.e., with decreasing viscosity) up to the crossing over point but enhances after that point and the temperature reduces in this case. Due to enhancement in thermal diffusivity parameter, temperature is observed to increase.

Natural convective flow past a horizontal cylinder with a muddy permeability medium in the presence of variable fluid properties was illustrated by Hassanien and Rashed[17]. Vajravelu *et al.*[18] studied the numerical solutions of unsteady laminar boundary layer flow of a viscous fluid at a vertical surface with diffusivity, viscosity and thermal radiation. They observed that the momentum and thermal boundary layer thickness decrease with the enhancement in the unsteady parameter. Srinivasacharya and Reddy[19] studied heat and mass transfer from a vertical plate embedded in a power-law fluid-muddy Darcy porous medium in the presence of chemical reaction and radiation effects.

In this analysis, we investigate the impacts of variable porosity, variable thermal conductivity, chemical reaction, Soret and Dufour on combined convective boundary layer flow, heat and mass transfer past a vertical plate immersed with permeable medium in a rotating system. The impact of the governing physical parameters, chemical reaction parameter, variable thermal conductivity, variable porosity, thermal diffusion and diffusion thermo effects on heat and mass transfer and a RK method with shooting technique is used for the solution purpose[19,20].

2 Mathematical Analysis

Figure 1 presents the geometry of the current problem under consideration. We consider steady, 2D laminar incompressible flow with heat and mass transfer throughout a porous vertical plate over a variable porosity medium in rotating system. Figure 1 embellished the physical model and coordinate system. Here x-axis is along the vertical plate and y-axis is normal to the surface. Consequently the free

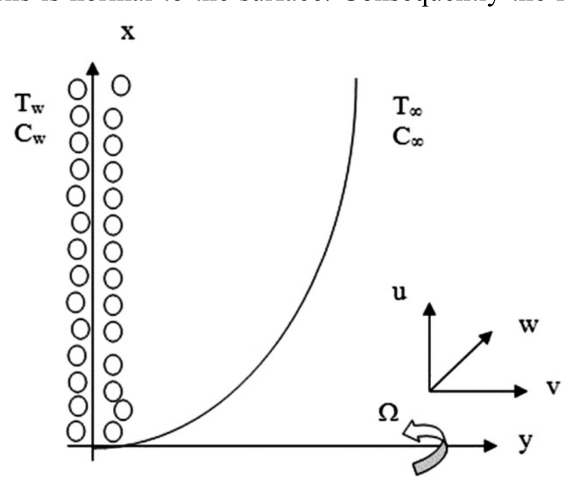

Fig. 1 – Physical model and coordinate system.

stream velocity u_∞ is parallel to the vertical plate and is constant. The plate is maintained at uniform temperature T_w and uniform concentration C_w which are higher than T_∞ and C_∞, respectively. Initially the plate is at rest and consequently the whole system is allowed to rotate in the presence of a constant angular velocity Ω about the y-axis. With accordance to facts sustained and inculcating Bousinessq approximations, the basic equations for the flow are:

$$\frac{\partial u}{\partial x}+\frac{\partial v}{\partial y}=0 \quad \dots(1)$$

$$\varepsilon^{-2}\left(u\frac{\partial u}{\partial x}+v\frac{\partial u}{\partial y}-2\Omega w\right)=\varepsilon^{-1}\upsilon\frac{\partial^2 u}{\partial y^2}+g\beta(T-T_\infty)+g\beta^*(C-C_\infty)-\frac{\sigma B_0^2}{\rho}u-\frac{\upsilon}{K}u \quad \dots(2)$$

$$\varepsilon^{-2}\left(u\frac{\partial w}{\partial x}+v\frac{\partial w}{\partial y}+2\Omega w\right)=\varepsilon^{-1}\upsilon\frac{\partial^2 w}{\partial y^2}-\frac{\sigma B_0^2}{\rho}w-\frac{\upsilon}{K}w \quad \dots(3)$$

$$u\frac{\partial T}{\partial x}+v\frac{\partial T}{\partial y}=\frac{\partial}{\partial y}\left(\alpha\frac{\partial T}{\partial y}\right)+\frac{D_m k_T}{c_s c_p}\frac{\partial^2 C}{\partial y^2}+\frac{Q_0}{\rho c_p}(T-T_\infty) \quad \dots(4)$$

$$u\frac{\partial C}{\partial x}+v\frac{\partial C}{\partial y}=D_m\frac{\partial^2 C}{\partial y^2}+\frac{D_m k_T}{T_m}\frac{\partial^2 T}{\partial y^2}-Kr^*(C-C_\infty) \quad \dots(5)$$

The corresponding boundary conditions are as given below:

$$u=0,\ \ v=\pm v(x),\ T=T_w,\ \ C=C_w\ \ at\ \ y=0$$
$$u\to u_\infty,\ T\to T_\infty,\ \ C\to C_\infty\ \ as\ \ y\to\infty \quad \dots(6)$$

The expressions for the constants involved in Eqs (1–6) are given in the Appendix.

We guess that α is differing as a linear function of the temperature in the mould[15]:

$$\alpha=\alpha_0(1+E(T_w-T_\theta))$$

where E being constant depending on the nature of the fluid and α_0 is the thermal diffusivity at the surface temperature T_w. In non-dimensional form:

$$\alpha=\alpha_0(1+\beta\theta) \quad \dots(7)$$

where $\beta=E(T_w-T_\infty)$ indicates the thermal conductivity parameter. Its range is define as:

$\beta=-0.1\le\beta\le 0$ for lubrication oil an $\beta=0\le\beta\le 0.12$ for water

Using Eq. (7), Eq. (4) becomes:

$$u\frac{\partial T}{\partial x}+v\frac{\partial T}{\partial y}=\alpha_0\frac{\partial}{\partial y}\left((1+\beta\theta)\frac{\partial T}{\partial y}\right)+\frac{D_m k_T}{c_s c_p}\frac{\partial^2 C}{\partial y^2}+\frac{Q_0}{\rho c_p}(T-T_\infty) \quad \dots(8)$$

Now we propose the following similarity variables:

$$\eta=y\sqrt{\frac{u_\infty}{\upsilon x}},\ \psi=\sqrt{\upsilon x u_\infty}\,f(\eta),\ \theta(\eta)=\frac{T-T_\infty}{T_w-T_\infty},$$
$$\phi(\eta)=\frac{C-C_\infty}{C_w-C_\infty},\ g=\frac{w}{u_\infty} \quad \dots(9)$$

where ψ be the stream function and $u=\frac{\partial\psi}{\partial y}$, $v=-\frac{\partial\psi}{\partial x}$ and η is similarity variable.

Using Eq. (9), Eqs (1–3), (5) and (8) become coupled non-linear ordinary differential equations as given below:

$$\varepsilon^{-1}f'''+\varepsilon^{-2}\left(\frac{1}{2}ff''+Rg\right)+Gr\theta+Gm\phi-(M+K)f'=0 \quad \dots(10)$$

$$\varepsilon^{-1}g''+\varepsilon^{-2}\left(\frac{1}{2}fg'-Rf'\right)-(M+K)g=0 \quad \dots(11)$$

$$(1+\beta\theta)\theta''+\beta(\theta')^2+\frac{1}{2}\Pr f\theta'+\frac{1}{2}\Pr Q\theta+\Pr Du\phi''=0 \quad \dots(12)$$

$$\phi''+\frac{1}{2}Scf\phi'-ScKr\phi+ScSo\theta''=0 \quad \dots(13)$$

The corresponding boundary conditions are:

$$f=f_w,\ \ f'=0,\ g=0,\ \theta=1,\ \ \phi=1\ \ at\ \eta=0 \quad \dots(14)$$

$$f'\to 1,\ \ g\to 0,\ \theta\to 0,\ \ \phi\to 0\ \ as\ \eta\to\infty \quad \dots(15)$$

where $R=\frac{4\Omega x}{u_\infty}$ rotational parameter, $K=\frac{2\upsilon x}{ku_\infty}$ Darcy number

$Gr=\frac{Gr_1}{\mathrm{Re}^2}$ temperature buoyancy parameter,

$M = \dfrac{\sigma B_0^2}{\rho u_\infty}$ magnetic parameter

$Gm = \dfrac{Gm_1}{\mathrm{Re}^2}$ mass buoyancy parameter, $\Pr = \dfrac{\upsilon}{\alpha_0}$ Prandtl number

$Gr_1 = \dfrac{g\beta(T_w - T_\infty)x^3}{\upsilon^2}$ Grashof number,

$Sc = \dfrac{\upsilon}{D_m}$ Schmidt number $Gm_1 = \dfrac{g\beta^*(C_w - C_\infty)x^3}{\upsilon^2}$ modified Grashof number, $Q = \dfrac{Q_0 x}{\upsilon \rho c_p}$ heat generation parameter

$Du = \dfrac{D_m k_T (C_w - C_\infty)}{c_s c_p (T_w - T_\infty)}$ Dufour number,

$S_0 = \dfrac{D_m k_T (T_w - T_\infty)}{\upsilon T_m (C_w - C_\infty)}$ Soret number

$Kr = \dfrac{Kr^*(C_w - C_\infty)2x}{u_\infty}$ chemical reaction parameter,

$f_w = \dfrac{2xv(x)}{\upsilon}\mathrm{Re}^{-1/2}$ dimensionless suction velocity.

3 Computational Solution

The reduced Eqs (10–13) are non-linear and their exact solutions are not possible. These are being resolved numerically applying RK45 order method for various values of parameters such as suction velocity, magnetic parameter, porosity parameter, thermal conductivity parameter, Dufour number, Soret number, heat generation, Prandtl number and chemical reaction. The impacts of the appearing parameters on the dimensionless primary velocity, secondary velocity, temperature, skin friction, the rates of heat and mass transfer are studied. The step size and convergence criteria were chosen to be 0.001 and 10^{-6}, respectively. The asymptotic boundary conditions in Eq. (15) were approximated by applying a value of 10 for η max as follows:

$$\eta_{\max} = 10, \quad f'(10) = 0, \quad g(10) = 0, \quad \theta(10) = 0, \quad \phi(10) = 0$$

This ensures that all numerical solutions approached the asymptotic values correctly.

4 Calculation of Local Skin Friction Coefficient, Nusselt Number and Sherwood Number

The skin-friction coefficient is denoted by:

$$\tau_x = \mu\left(\frac{\partial u}{\partial y}\right)_{y=0} \quad \text{and} \quad \tau_z = \mu\left(\frac{\partial w}{\partial y}\right)_{y=0}$$

which are proportional to $\left(\dfrac{\partial^2 f}{\partial \eta^2}\right)_{\eta=0}$ and $\left(\dfrac{\partial g}{\partial \eta}\right)_{\eta=0}$ … …(16)

The Nusselt number is denoted by:

$$Nu = -\frac{1}{\Delta T}\left(\frac{\partial T}{\partial y}\right)_{y=0}$$

and the Sherwood number is denoted by:

$$Sh = -\frac{1}{\Delta C}\left(\frac{\partial C}{\partial y}\right)_{y=0}$$

and these parameters in non-dimensional form:

$$Nu = \left(\frac{\partial \theta}{\partial \eta}\right)_{\eta=0} \quad \text{and} \quad Sh = \left(\frac{\partial \phi}{\partial \eta}\right)_{\eta=0}$$

To demonstrate, the current solution, similarity has been established with already publicized data from the literature for skin friction, local Nusselt number and local Sherwood number in Table 1, and they are observed to be in a appreciative concurrence. Table 2 shows the impacts of the skin- friction coefficient, Nusselt number, and Sherwood number for various values of relevant parameters.

5 Results and Discussion

In this article, the influences of heat and mass transfer on magnetohydrodynamic (MHD) incompressible fluid past a vertical plate in a rotating system with heat source and chemical reaction have been investigated. Numerical computations for velocity and temperature are obtained by using R-K–Fehlberg fourth-5th order with shooting method. The outcomes of the present work are compared with the results of Bhuvanavijaya and Mallikarjuna[22] in the non-appearance absence of magnetic parameter ($M = 0$) as shown in Table 1.

Figure 2 shows the velocity distribution for different values of suction parameter. It is noted that the velocity profile increases rapidly near the plate and the boundary layer became thin within the region

Table 1 — Comparison of skin friction coefficient, Nusselt and Sherwood numbers for various values of Du and S_0 at $\Pr = 0.71, G_r = 1, G_m = 0.1, f_w = 0.5, Sc = 0.22$ and remaining parameters are zero.

Parameters		Alam and Rahman[21]			Bhuvanavijaya and Mallikarjuna[22]			Present results		
Du	S_0	Cf	Nu	Sh	Cf	Nu	Sh	Cf	Nu	Sh
0.030	2.0	1.6795	0.5310	0.1292	-	0.5309	0.1288	1.6568	0.5279	0.1275
0.037	1.6	1.6758	0.5299	0.1605	-	0.5301	0.1602	1.6531	0.5268	0.1587
0.050	1.2	1.6724	0.5285	0.1921	-	0.5289	0.1920	1.6500	0.5255	0.1901
0.060	1.0	1.6712	0.5275	0.2077	-	0.5270	0.2075	1.6488	0.5246	0.2055
0.075	0.8	1.6707	0.5263	0.2233	-	0.5258	0.2230	1.6483	0.5233	0.2211
0.120	0.5	1.6723	0.5230	0.2470	-	0.5225	0.2465	1.6501	0.5201	0.2447
0.600	0.1	1.7218	0.4908	0.2817	-	0.4905	0.2812	1.7006	0.4897	0.2794

Table 2 — Numerical values of skin friction coefficient, Nusselt and Sherwood numbers for various values of parameters when $\Pr = 0.71, G_r = 1, G_m = 0.1, f_w = 1, Sc = 0.22, \varepsilon = 2$.

M	β	Kr	Du	S_0	Q	Cf	Nu	Sh
0	0.2	0.3	0.2	0.2	0.1	2.1269	-0.5134	-0.3941
0.5						1.4907	-0.4192	-0.3577
1						1.2306	-0.3760	-0.3468
	0.5					1.2662	-0.3170	-0.3514
	1					1.3098	-0.2570	-0.3570
	2					1.3649	-0.1947	-0.3642
		0.5				1.3631	-0.1915	-0.4272
		0.8				1.3610	-0.1875	-0.5063
		1				1.3599	-0.1852	-0.5523
			0.3			1.3670	-0.1754	-0.5529
			0.5			1.3811	-0.1557	-0.5541
			0.8			1.4020	-0.1262	-0.5558
				0.5		1.4019	-0.1259	-0.5576
				1		1.4018	-0.1253	-0.5607
				1.5		1.4017	-0.1247	-0.5639
					0.3	1.4441	-0.0690	-0.5780
					0.6	1.5214	0.0326	-0.6034
					1	1.6548	0.2124	-0.6483

up to η =2 and then it tends to be constant to meet inadequate boundary condition. So far as effect of suction is concerned velocity profile increases as the suction parameter increases. Figure 3 presents the impact of suction on temperature profile. It is clear to observe that temperature profile decreases up to the thermal boundary region of η =5 and after that the trend is constant to meet the boundary condition. Further, it is noticed that as suction increases the temperature reduces at all points in the thermal boundary layer. Similar effect is encountered for the concentration profile as shown in the Fig. 4 which represents the effect of suction on concentration distribution. It is noteworthy that concentration decreases up to η =5 and then it tends to be constant and profile is parabolic in nature. So far as effect of suction is concerned with increase in suction parameter the concentration decreases.

Figure 5 exhibits the velocity distribution for different values of magnetic parameter *M*. It is observed that the present result is in good agreement with the result of Bhuvanavijaya and Mallikarjuna[22] in the non-appearance of magnetic parameter ($M = 0$). Further, velocity profile decreases in the presence of magnetic field. It is a well established result since the interaction of magnetic field produces a resistive force which reduces the momentum in the velocity boundary layer and hence the velocity decreases.

Figures 6 and 7 display the variation of temperature and concentration distributions for various values of *M*. Both the profiles increase up to the region η =5 and η =8, respectively and then trend

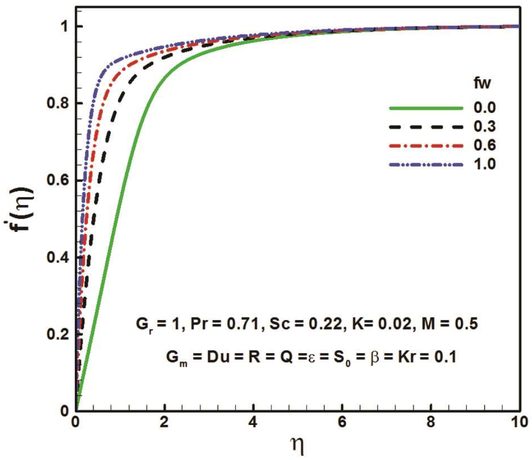

Fig. 2 – Velocity profiles for dissimilar values of suction.

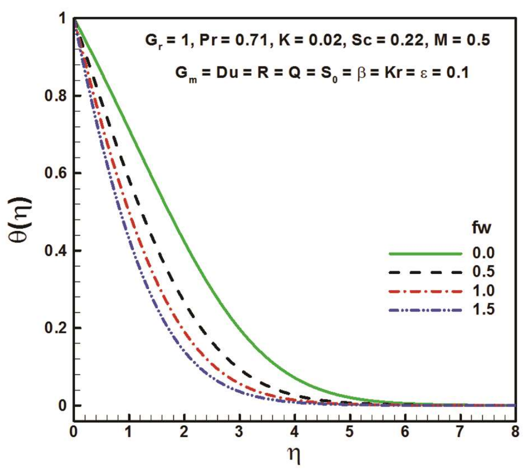

Fig. 3 – Temperature profiles for dissimilar values of suction.

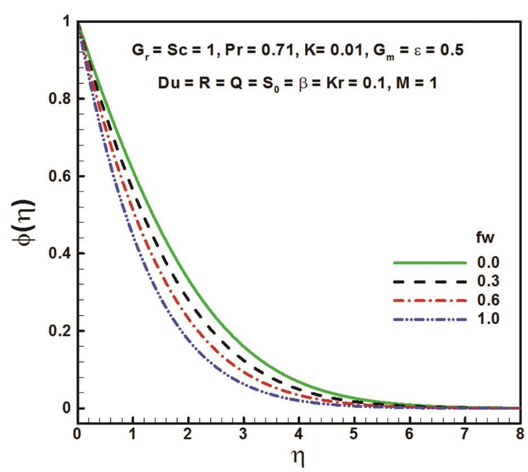

Fig. 4 – Concentration description for dissimilar values of suction.

is uniform to meet inadequate boundary conditions. Thus, it is concluded that magnetic parameter enhances the temperature. To justify this outcome, it is to note that resistance offered by magnetic

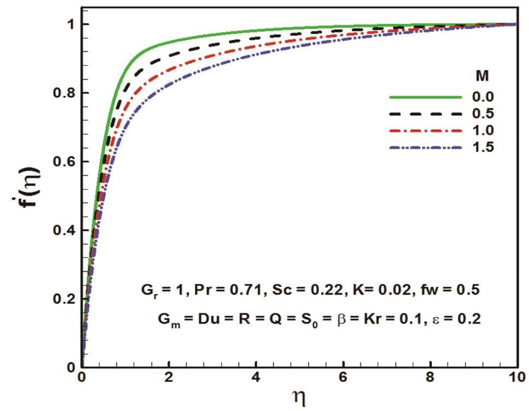

Fig. 5 – Velocity profiles for dissimilar values of magnetic parameter.

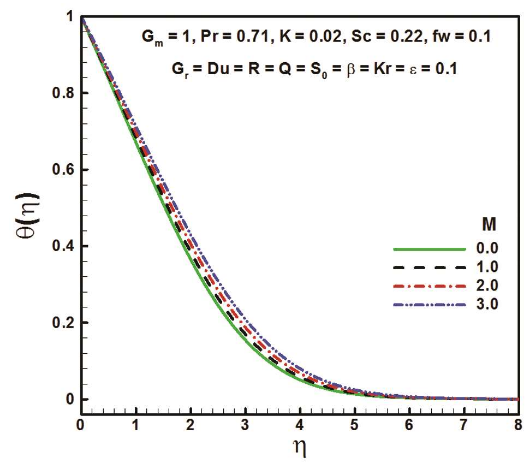

Fig. 6 – Temperature profiles for dissimilar values of magnetic parameter.

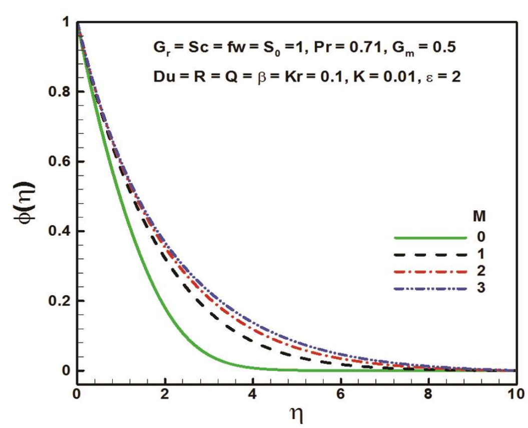

Fig. 7 – Concentration profiles for dissimilar values of magnetic parameter.

parameter contributes to reducing momentum (velocity) generates heat and mass so that temperature and concentration increases.

Figure 8 illustrates the effect of porosity regime ε on the velocity boundary layer. It is quite interesting to observe that increasing values of porosity regime ε the fluid velocity increases resulted in the boundary layer thickness also increases.

Figure 9 exhibits the temperature profiles for different values of *Q*. It is to note that enhance in heat generation parameter (*Q*), temperature profiles increases. Consequently, work done for squeezing the thickness converted to heat energy as a result of which temperature increases.

Figure 10 displaces the concentration distribution with Kr . It is seen that appearance of Kr, reduces the concentration profile in the corresponding boundary layer significantly.

The skin friction is the measure of shear stress at the plate. Figure 11 shows the impact of magnetic parameter, porosity and the suction on skin friction. It is observed that increase in suction, porosity and magnetic parameter, the skin friction coefficient reduces.

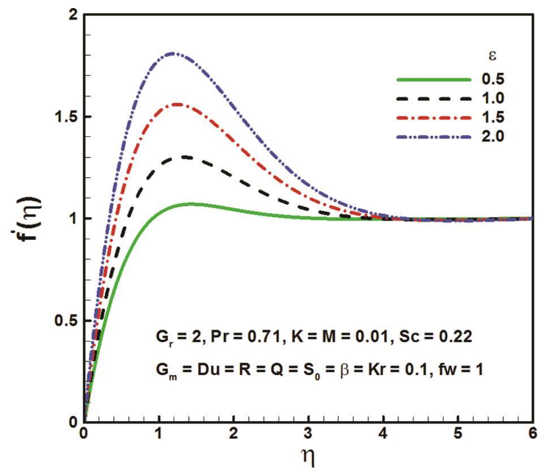

Fig. 8 – Velocity profiles for dissimilar values variable porosity regime.

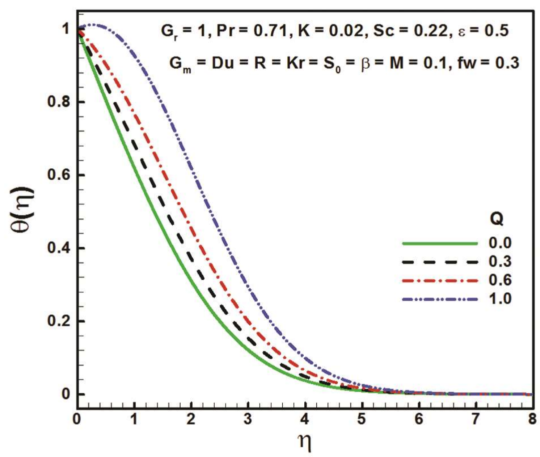

Fig. 9 – Temperature profiles for dissimilar values of heat generation parameter.

Figure 12 exhibits the impact of rate of heat transfer for different values of magnetic parameter, porosity and suction. It is observed that rate of heat transfer is maximum in the absence of suction. Further, it represents three layer characteristic in the flow domain with an increase in magnetic parameter. Moreover, suction and porosity both are desirable for reduction of rate of heat transfer.

Figure 13 exhibits the variation of magnetic parameter with various values of mass buoyancy and variable thermal conductivity on rate of mass transfer profile. It is interesting to note that the rate of mass transfer reduces due to increase in mass buoyancy parameter. Again the distinct two layer variation indicates that increase in variable thermal conductivity is favorable to reduce the rate of mass transfer.

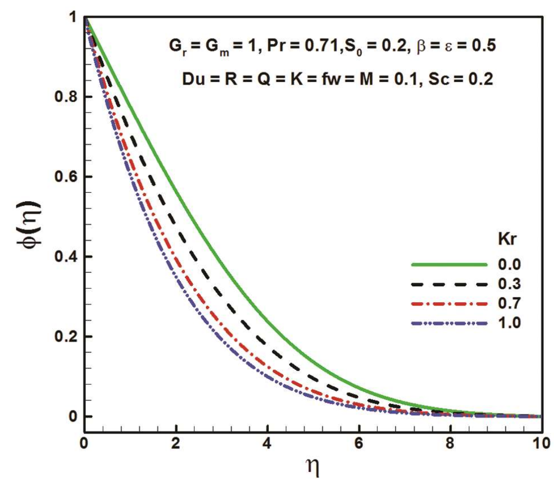

Fig. 10 – Concentration profiles for dissimilar values of chemical reaction parameter.

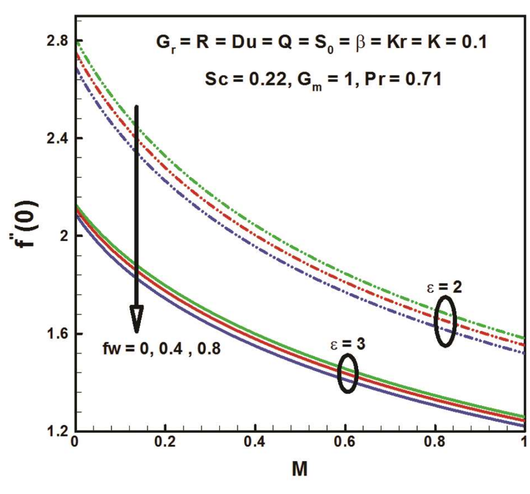

Fig. 11 – Effects of M, ε and f_w on skin friction coefficient.

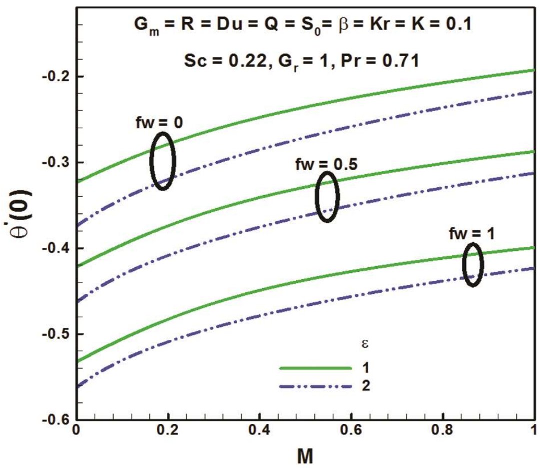

Fig. 12 – Effects of M, ε and f_w on heat transfer rate.

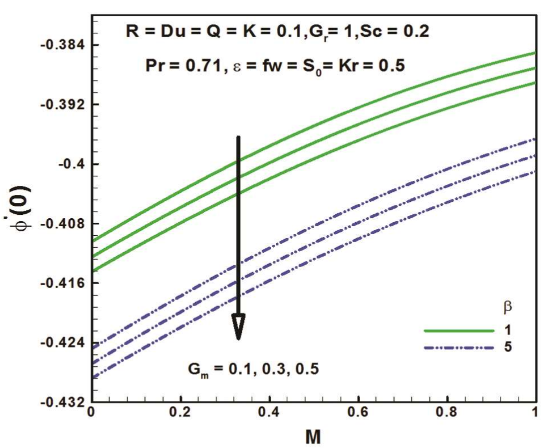

Fig. 13 – Effects of G_m, β and M on mass transfer rate.

6 Conclusions

The velocity profile of fluid flow enhances with the enhancement in suction parameter whereas the temperature and concentration profile decreases with an increase in suction parameter. Velocity profile decreases in the presence of magnetic field but the magnetic parameter enhances the temperature and concentration profiles. An enhancing porosity regime ε outcomes an increasing in velocity description. On the enhancement in heat generation parameter (Q), the temperature profile increases. Rate of heat transfer is maximum in the absence of suction. Moreover, suction and porosity both are desirable for reduction of rate of heat transfer. The value of skin friction reduces with an increase in suction, porosity and magnetic parameter. The rate of mass transfer reduces due to increase in mass buoyancy parameter.

Acknowledgement

The authors are grateful to Prof G C Sharma, Agra University, Agra, India for his help and valuable suggestions to prepare this research paper and thanks to reviewers also.

Nomenclature

C: Fluid Concentration
k : permeability
Du : Dufour number
$\Pr$: Prandtl number
S_0 : Soret number
g : acceleration due to gravity
M : Magnetic parameter
Kr^* : chemical reaction rate
D_m : Coefficient of mass diffusivity

Greek symbols

Sc : Schmidt number
$\theta(\eta)$: dimensionless temperature
T : Fluid temperature
μ: dynamic viscosity
T_∞ : Fluid temperature at infinity
ε : porosity
B_0 : Magnetic flux density
α : thermal diffusivity
Sh : Sherwood number
σ : Electrical conductivity
Nu : Nusselt number
ρ : density
Kr : Chemical reaction parameter
υ : kinematic viscosity
C_∞ : Species concentration at infinity
β : thermal expansion coefficient
c_p : Specific heat at constant pressure
β^* : concentration expansion coefficient
c_s : Concentration susceptibility
Ω : angular velocity
R : Rotational parameter
η : similarity variable
k_T : Thermal diffusion ratio
Q_0 : Volumetric rate of heat generation
T_m : mean temperature of the fluid
Q : Heat generation parameter
Re : Reynolds number
x, y, z : coordinates
u, v, w : Velocity constituents along $x, y \, and \, z$ direction

References

1 Mathers W G, Madden A J & Piret E L, *Ind Eng Chem*, 49 (1957) 961.
2 Chapman S & Cowling T G, *The mathematical theory of non-uniform gases*, (Cambridge University Press: UK), 1952.
3 Anwar Beg O, Takhar H S, Beg T A, Chamkha A J, Nath G & Majeed R, *Int J Fluid Mech Res*, 32 (2005) 383.
4 Al-Humoud J M & Chamkha A J, *Int J Heat Tech*, 24 (2006) 51.
5 Mbeledogu I U & Ogulu A, *Int J Heat Mass Trans*, 50 (2007) 1902.
6 Anwar Beg O, Takhar H S, Zueco J, Sajid A & Bhargava R, *Acta Mech*, 200 (2008) 129.
7 Salah F, Aziz Z A & Ching D L C, *J Appl Math*, 1 (2011) 53.
8 Schwartz C E & Smith J M, *Ind Eng Chem*, 45 (1953) 1209.
9 Vafai K & Tien C L, *Int J Heat Mass Trans*, 24 (1981) 195.
10 Pal D & Mondal H, *Acta Mech*, 44 (2009) 133.
11 Pal D, *Commun Nonlinear Sci Numer Simul*, 15 (2010) 3974.
12 Prasad V R, Vasu B, Anwar Beg O & Parshad R D, *Commun Nonlinear Sci Numer Simul*, 17 (2012) 654.
13 Vedavathi N, Ramakrishna K & Jayarami Reddy K, *Ain Shams Eng J*, 6 (2015) 363.
14 Alao F I, Fagbade A I & Falodun B O, *J Nigerian Math Soc*, 35 (2016) 142.
15 Seddeek, M A & Salama F A, *Comput Mater Sci*, 40 (2007) 186.
16 Mukhopadhyay S, *Int J Heat Mass Trans*, 52 (2009) 5213.
17 Hassanien I A & Rashed Z Z, *Commun Nonlinear Sci Numer Simul*, 16 (2011) 1931.
18 Vajravelu K, Prasad K V & Chiu N G, *Anal Real World Appl*, 14 (2013) 455.
19 Srinivasacharya D & Swamy R G, *Heat Trans Asian Res*, 42 (2013) 485.
20 Narayana M, Khidir A A, Sibanda P & Murthy P V S N, *Transport Porous Med*, 96 (2013) 419.
21 Alam M S & Rahman M M, *Nonlinear Anal Model Control*, 11 (2006) 78.
22 Bhuvanavijaya R & Mallikarjuna B J, *Naval Arch Marine Eng*, 11 (2014) 83.